Hiroshima University Doctoral Thesis

Targeted mutagenesis using CRISPR-Cas9 in sea urchin, *Hemicentrotus pulcherrimus*

(バフンウニにおける CRISPR-Cas9 を用いた標的遺伝子への変異導入)

2020

Department of Mathematical and Life Sciences,
Graduate School of Science,
Hiroshima University

Liu Daming

Table of Contents

1. Main Thesis

Targeted mutagenesis using CRISPR-Cas9 in sea urchin, *Hemicentrotus pulcherrimus*

(バフンウニにおける CRISPR-Cas9 を用いた標的遺伝子への変異導入)

2. Article

Establishment of knockout adult sea urchins by using a CRISPR-Cas9 system.

Liu, D., Awazu, A., Sakuma, T., Yamamoto, T., & Sakamoto, N.

Development, growth & differentiation, 61(6), 378-388, 2019.

Main Thesis

Targeted mutagenesis using CRISPR-Cas9 in sea urchin, *Hemicentrotus pulcherrimus*

Liu Daming

Department of Mathematical and Life Sciences

Graduate School of Science

Hiroshima University

2020

Contents

Introduction

Sea urchins are invertebrate deuterostomes, which is a sister group of the chordates. Investigation of the sea urchin genome is important to understand the origin of vertebrate gene functions. Sea urchins are a model organism for research on developmental biology. The fertilized eggs and embryos of sea urchin can be manipulated directly because of its simple organization. It is therefore very suitable for studies of developmental process such as morphogenetic movements, cell interactions, changes in gene expression associated with the establishment of tissue territories (Becker et al., 2003). Furthermore, sea urchin has been recently used for the analysis of gene regulatory networks during early development (Davidson et al., 2002; Oliveri & Davidson, 2004; Oliveri et al., 2008).

Although deuterostomes generally have bilateral bodies, the bilateral body plan of sea urchin embryos and larvae is converted to a pentameral body plan after metamorphosis. The metamorphosis of sea urchin is a complex developmental progression, much of which takes place in the adult rudiment produced from the left side of the coelomic pouch that originates from small micromere and macromere descendants (Cameron et al., 1991; Cameron et al., 1987).

The first sea urchin genome sequenced was that of *Strongylocentrotus purpuratus* (Sea Urchin Genome Sequencing Consortium, 2006). *Hemicentrotus pulcherrimus*, which is closely related to *S. purpuratus*, is widely distributed in Japan and has also been used for research on developmental biology. The *H. pulcherrimus* genome was deciphered in 2018 (Kinjo et al., 2018). The genome size of *H. pulcherrimus* was estimated to be 800 Mbp, with approximately 25,000 genes.

Analysis of gene function in the sea urchin embryo has relied on gene knockdown by morpholino antisense oligonucleotide (MASO), which blocks translation or RNA splicing of gene transcripts of interest (Angerer & Angerer, 2004). However, the effect of MASO-mediated knockdown is not long lasting. Therefore, it is impossible to perturb gene expression during late developmental stages by MASO.

Genome editing is a type of genetic engineering technology which enables deletion, insertion and replacement of DNA at a targeted locus within the genome using programmable nucleases. These nucleases enable efficient genetic modifications by inducing double strand breaks (DSBs) at a precise position and subsequent repair of DSBs. Currently, three types of programmable nucleases have mainly been used: zinc finger nuclease (ZFN), transcription activator-like effector nuclease (TALEN) and clustered regularly interspaced short palindromic repeat (CRISPR)-CRISPR-associated nuclease 9 (Cas9) system. Unlike the first two technologies, which use proteins to target nucleotide sequences, CRISPR-Cas9 system utilizes a short RNA segment as a guide, increasing the ease of experimental manipulation (Gaj et al., 2013).

In recent years, genome editing technologies have been used in sea urchin embryos to knockout genes that are expressed during early development (Hosoi et al., 2014; Lin & Su, 2016; Mellott et al., 2017; Ochiai et al., 2010; Oulhen et al., 2017; Oulhen & Wessel, 2016). Upon targeted genome editing using zinc-finger nuclease (ZFN) in *H. pulcherrimus* embryos, approximately 10% of ZFN mRNA-injected embryos showed an affected phenotype (Ochiai et al., 2010). Upon targeted genome editing with transcription activator-like effector nuclease (TALEN) in *H. pulcherrimus* embryos, 12.6% of TALEN pair-injected embryos showed an affected phenotype (Hosoi et al., 2014). These rates of the affected phenotypes are not satisfactory, and a higher mutagenesis efficiency is indispensable for detailed analysis of gene functions of *H. pulcherrimus*.

CRISPR-Cas9 is a microbial adaptive immune system which use RNA-guided nucleases to cleave invading foreign DNA (Horvath & Barrangou, 2010). The most widely used type II CRISPR-Cas9 system is derived from *Streptococcus pyogenes*. Foreign DNA is integrated within the CRISPR genomic locus, transcribed and processed into CRISPR RNA (crRNA). crRNA then anneal to trans-activating crRNA (tracrRNA) which is critical for crRNA maturation and recruiting the Cas9 nuclease to DNA. crRNA and tracrRNA can be fused by a short linker to form a single guide RNA (sgRNA). sgRNA and Cas9 nuclease form a complex to scan the genome for protospacer adjacent motif (PAM), which is NGG for the type II *Streptococcus pyogenes* Cas9 (SpCas9). SpCas9 endonuclease mediates a DSB 3-bp upstream of the PAM site. By re-designing

the crRNA, CRISPR-Cas9 system can thereby be re-targeted to cleave virtually any DNA sequence.

Compared to ZFN and TALEN, which rely on protein/DNA recognition, the CRISPR-Cas9 system uses a single guide RNA (sgRNA), which is more efficient, convenient, and cost-effective (Doudna & Charpentier, 2014). Targeted genome editing using a CRISPR-Cas9 system has been reported in *S. purpuratus* (Lin & Su, 2016; Mellott et al., 2017; Oulhen & Wessel, 2016; Oulhen et al., 2017), but not in *H. pulcherrimus.* Furthermore, the effect of genome editing in adult sea urchin after metamorphosis has never been studied.

Nodal is a member of the Transforming Growth Factor beta (TGFβ) superfamily, and it has been reported that knockdown of Nodal by MASO disrupts the dorsoventral axis and radializes the embryos in sea urchin (Duboc et al., 2004).

Polyketide synthases (PKSs) are a large group of enzymes responsible for the biosynthesis of polyketide compounds (Castoe, et al., 2007; Hopwood, 1997; Hopwood & Sherman, 1990; Staunton & Weissman, 2001). Sea urchins have two PKS genes, *Pks1* and *Pks2* (Castoe et al., 2007). The onset of *Pks1* expression occurs in the blastula stage, and *Pks1* expression is restricted to secondary mesenchyme cell (SMC) precursors at the vegetal pole of the embryo and larval pigment cells, which are derived from SMCs (Barsi et al., 2015; Calestani et al., 2003). *Pks1* is required for the biosynthesis of the naphthoquinone pigment echinochrome, (Griffiths, 1965). Knockdown of *Pks1* by MASO resulted in albino embryos (Calestani et al., 2003). *Pks2* expression is restricted to skeletogenic cells and their precursors (Beeble & Calestani, 2012), and *Pks2* plays a critical role in the formation of calcareous larval skeletons (Hojo et al., 2015).

The specification of the pigment cell is initiated by the activation of the gene encoding the transcription factor Gcm by Delta signaling received from the skeletogenic mesoderm (Materna et al., 2013; Ransick & Davidson, 2006; Croce & McClay, 2010; Peterson & McClay, 2005). According to studies in *S. purpuratus*, Gcm activates *GataE* and *Pks1* and feeds back to its own gene activation. GataE activates *Pks1* and *Six1/2*; then Six1/2 feeds back to activate *Gcm* (Ransick & Davidson, 2006, 2012; Materna, et

al., 2013; Lee & Davidson, 2004; Lee et al., 2007).

In this thesis, to establish a highly efficient method for genome editing in *H. pulcherrimus*, I examined the feasibility of CRISPR-Cas9 system in *H. pulcherrimus*, I targeted *H. pulcherrimus Nodal* (*HpNodal*) gene and evaluated the efficiency of mutagenesis. High mutation rate was observed in sgRNA-injected embryos within 24 hr post fertilization (hpf), indicating that CRISPR-Cas9 system can be used in *H. pulcherrimus* to induce mutations efficiently. Moreover, using this efficient gene knockout method, I targeted *H. pulcherrimus Pks1* (*HpPks1*) that is known to be related to embryonic pigmentation in sea urchin. High-efficiency mutagenesis was detected and an albino phenotype was observed in sgRNA-injected embryos. The albino phenotype was maintained in adult sea urchins after metamorphosis, indicating successful establishment of knockout adult sea urchin. These results suggest that the CRISPR-Cas9 system is an effective gene knockout technology in *H. pulcherrimus* and can be used for the analysis of late developmental processes.

Materials and Methods

Sea urchin culture

Adult sea urchins (*H. pulcherrimus*) were collected from the Seto Inland Sea or Tateyama Bay. Eggs and sperm were obtained by coelomic injection of 0.55 M KCl. Fertilized eggs were cultured in filtered seawater at 16°C. Larvae were fed the microalgae *Chaetoceros gracilis* and were cultured under rotation. *C. gracilis* was purchased from I.S.C. Co., Ltd. and cultured in filtered seawater supplemented with 1/1,000 volume of marine algae culture medium (KW21; Daiichi Seimo Co., Ltd.) and sodium metasilicate at 16°C under continuous illumination and aeration. After the metamorphosis, juvenile sea urchins were fed dried kelp and natural microalgae attached on oyster shells and cultured at 16°C.

Preparation sgRNA

SgRNAs targeting *Nodal* were designed using CRISPR-direct (Naito et al., 2014). SgRNAs targeting *Pks1* were designed following Oulhen and Wessel (2016). Templates for sgRNA synthesis were assembled by a PCR-based strategy (Nakayama et al., 2014; Sakane et al., 2017). Briefly, sgRNA-fwd and reverse-sgRNA were annealed and served as primers for fill-in extension, and the resulting template was amplified with T7-sgRNA-fwd and sgRNA-rev using KOD FX Neo (Toyobo) and purified using a QIAquick PCR Purification Kit (Qiagen). Subsequently, sgRNAs were transcribed using a MEGAshortscript T7 Kit (Thermo Fisher Scientific) and purified using a RNeasy Mini Kit (Qiagen). The oligonucleotide information used is listed in Table 1.

Preparation mRNA

Humanized codon-optimized *SpCas9* cDNA from pX330 (plasmid #42230, Addgene; Cong et al., 2013) was subcloned into a pGreenLantern-derived plasmid, and

two SV40 nuclear localization signals were inserted at the 3′ end of the *SpCas9* sequence. After linearization of this vector with *SpeI*, *SpCas9* mRNA was synthesized using an mMESSAGEmMACHINE T7 Ultra kit (Thermo Fisher Scientific) and purified using a RNeasy Mini Kit.

Microinjection of sgRNA and *SpCas9* mRNA

Microinjection was carried out as described by Rast (2000) with some modifications. *SpCas9* mRNA and sgRNA were dissolved in 30% glycerol at 750 and 150 ng/µl, respectively, and two pl of RNA solution was microinjected into fertilized eggs.

Images of larvae were acquired with an epifluorescence microscope BX50 (Olympus) equipped with a DP72 digital camera and analyzed with DP2-BSW software (Olympus). To obtain a focused image of each larva, Z-stacks of each individual embryo were processed in FIJI software using the Stack Focuser plug-in. After metamorphosis, images of juvenile and adult sea urchins were acquired with a JVC GC-PX1 digital camera (Victor Corporation) mounted on a Leica MZ75 stereo microscope (Leica).

Isolation of genomic DNA

Genomic DNA was isolated using a simple method described by Lin and Su (2016). At 24 hpf, 20 embryos were incubated in 8 µl of lysis buffer (1× NEB#2 buffer; New England Biolabs) at 94°C for 10 min, and then cooled down to 4°C for 10 min. After addition of 1 µl of 18.6 mg/ml proteinase K, PCR Grade (Roche), the sample was incubated at 55°C for 2 hr. After subsequent incubation at 94°C for 10 min to inactivate proteinase K, 8 µl of TE buffer (10 mM Tris-HCl (pH 8.0), 1 mM EDTA) was added for use in PCR.

For extraction of genomic DNA from whole 5-month-old adult sea urchin, an individual sea urchin was added to 30 µl of lysis buffer in a 1.5-ml tube and homogenized. After incubation at 94°C for 10 min and then at 4°C for 10 min, 1 µl of 18.6 mg/ml proteinase K was added and the sample was incubated at 55°C for 2 hr. After inactivation

of proteinase K, 30 μl TE buffer was added.

Heteroduplex mobility assay (HMA)

For HMA, target regions were amplified from 1 μl of isolated genomic DNA solution in 35 PCR cycles using KOD FX Neo. The PCR products were analyzed using an MCE-202 MultiNA (Shimadzu) or a 0.5% agarose gel supplemented with resolution enhancer (patent applied; Dr. Masanobu Obara in Hiroshima University, GeLBio LLC) or 3% agarose gel in 1×TAE buffer (40 mM Tris–acetate, 1 mM EDTA) with mini-sized gel electrophoresis apparatus (Mupid, ADVANCE Co., Ltd.) and stained with ethidium bromide. Nucleotide sequences of the primers used to amplify each target region are listed in Table 2.

DNA sequencing analysis

For Sanger sequencing, PCR products obtained by 27 PCR cycles were subcloned into the pBluescript SK(-) vector or pTA2 vector (TArget Clone -Plus-; Toyobo). Positive clones were detected by colony PCR and sequenced with the M13 forward or M13 reverse primer using a BigDye Terminator v3.1 Cycle Sequencing Kit (Thermo Fisher Scientific).

Whole mount in situ hybridization (WMISH)

The cDNA fragments encoding the *HpPks1* and *HpGcm* homologue of *H. pulcherrimus* was amplified by PCR with the primers listed in Table 2. PCR products obtained by 27 PCR cycles were subcloned into the pTA2 vector (TArget Clone -Plus-). After linearization with restriction endonuclease, these plasmids were used as templates for syntheses of RNA probes. Sense and antisense DIG-labeled RNA probes were synthesized using DIG RNA Labeling Mix (Roche, Switzerland) with either T7 or T3 RNA polymerase (Roche).

WMISH was carried out as described by Minokawa et al. (2004) with some modifications. At the gastrula larva stages, embryos were fixed overnight with 4% paraformaldehyde, 32.5% filtered seawater, 32.5 mM MOPS (pH 7.0) and 162.5 mM NaCl at 4 °C, before storage in 99% ethanol at 20 °C. Rehydration of specimens was followed by prehybridization in hybridization buffer [70% formamide, 0.1 M MOPS (pH 7.0), 0.5 M NaCl, 0.1% Tween-20, and 1 mg/mL BSA] and hybridization in hybridization buffer containing 0.1 ng/ul digoxigenin-labeled probe at 50 °C for 5 days. Hybridized probe was immune-detected with alkaline phosphatase-conjugated anti-digoxigenin antibody (Roche, Switzerland), and the chromogenic staining was carried out with BCIP (5-bromo-4-chloro-3-indolyl phosphate; Roche, Switzerland) and NBT (nitro blue tetrazolium; Roche).

Quantitative reverse transcription PCR (qRT-PCR) analysis

Total RNA was extracted from embryos at different stage by ISOGEN (Nippongene, Japan), purified by RNeasy mini kit (QIAGEN, Germany) and used for cDNA synthesis using ReverTra Ace@ qPCR RT Master Mix with gDNA Remover (TOYOBO, Japan). The resulting cDNA was used as template for qRT-PCR by KOD SYBR qPCR Mix (TOYOBO, Japan) with the primers listed in Table 2. The qRT-PCR analysis was carried out using Step One real-time PCR system (Thermo Fisher Scientific), and the level of *HpPks1* and *HpGcm* mRNA expression was normalized by that of *mitochondrial cytochrome oxidase subunit I* (*MitCOI*) expression, which is expressed constitutively at the same level during sea urchin development (Okabayashi & Nakano, 1983; Yamaguchi et al., 1994; Fujiwara & Yasumasu, 1997).

Results

CRISPR-Cas9-mediated mutagenesis of *HpNodal*

To validate the feasibility of genome editing with CRISPR-Cas9 system in the sea urchin *H. pulcherrimus*, I targeted Nodal homolog of *H. pulcherrimus* (*HpNodal*) gene. Knockout of *Nodal* has been reported to result in radialized phenotype in the closely related sea urchin species, *S. purpuratus* (Lin & Su, 2016).

In this study, I tested two sgRNAs targeting each exon of *HpNodal*, respectively (Figure 1a, b). The sgRNAs were microinjected with *SpCas9* mRNA into fertilized eggs of *H. pulcherrimus*, and genomic DNA was extracted at 24 hpf from 20 embryos injected with SpCas9/sgRNA or SpCas9 alone. CRISPR-Cas9-mediated mutagenesis was examined by HMA. The PCR product from embryos injected with sgRNA#1 shows shifted bands representing heteroduplexes formed by mutated alleles, compared to SpCas9 alone (control) (Figure 1c). While the PCR product from embryos injected with sgRNA#2 shows no difference from the control.

To analyze the types and efficiency of mutations induced by CRISPR-Cas9-mediated genome editing, the PCR amplicons were subcloned and sequenced. Among 20 sequenced clones from sgRNA#1-injected embryos, deletions (10 clones) and insertion (3 clones) were observed, indicating that the mutation rate was 65% (Figure 2a) and the frameshift rate was 30%. On the other hand, among 20 sequenced clones from sgRNA#2-injected embryos, only 2 clones showed deletion (Figure 2b), which is consistent with the HMA results (Figure 1c). Furthermore, deletions seemed to be caused not only by nonhomologous-end joining (NHEJ), but also by microhomology-mediated end joining (MMEJ; Figure 2, underline).

Radialized phenotype in *HpNodal* sgRNA-injected embryos

I examined the phenotype of the sgRNA-injected embryos. All the control embryos

injected with *SpCas9* mRNA alone developed normally (Figure 3a, b). The sgRNA#2-injected embryos also developed normally and were morphologically indistinguishable from control embryos (data not shown). However, when sgRNA#1 was injected, abnormal skeletogenesis and radialized shape was observed in larvae at the prism stage (Figure 3c, d). These results indicated that the *HpNodal* gene was disrupted in the SpCas9/sgRNA#1-injected embryos and CRISPR-Cas9 can be used for the analysis of early developmental processes in *H. pulcherrimus*.

CRISPR-Cas9-mediated mutagenesis of *HpPks1*

To further evaluate the functionality of the CRISPR-Cas9 system in *H. pulcherrimus*. I targeted the *H. pulcherrimus* polyketide synthase *Pks1* (*HpPks1*) because knockout of *Pks1* produces an easily observable albino phenotype as recently reported in the closely related sea urchin species, *S. purpuratus* (Oulhen & Wessel, 2016). To obtain the nucleotide sequence of *HpPks1*, I searched the *H. pulcherrimus* Genome and Transcriptome database (HpBase, http://cell-innovation.nig.ac.jp/Hpul/) and I found that the *HpPks1* locus is located on scaffold 824.

First, I examined the temporal and spatial expression patterns of *HpPks1* gene during early development of *H. pulcherrimus*. To analyze the temporal expression of *HpPks1* in *H. pulcherrimus*, I pooled thousands of *H. pulcherrimus* embryos at various developmental stages from the hatched blastula (10 hpf) through to pluteus larva (1week post fertilization), and measured the *HpPks1* mRNA levels by qRT-PCR. The onset of *Pks1* expression occurs at the early blastula stage (Figure 4a). The expression pattern of *HpPks1* in *H. pulcherrimus* is similar to that in *S. purpuratus* (Materna et al., 2010).

To examine the spatial expression pattern of *HpPks1* in *H. pulcherrimus*, WMISH was performed with embryos at mesenchyme blastula and late gastrula stages. The expression of *HpPks1* mRNA was restricted to presumptive secondary mesenchyme cells (SMCs) and SMCs (Figure 4b, c).

For CRISPR-Cas9-mediated mutagenesis in *HpPks1* gene, I tested three sgRNAs targeting the second coding exon of *HpPks1* (Figure 5a and 6) that correspond to those

used in *S. purpuratus* (Oulhen & Wessel, 2016). Although the preceding study using *S. purpuratus* introduced a combination of three sgRNAs (Oulhen & Wessel, 2016), I used each single sgRNA in this study. The sgRNAs were microinjected with SpCas9 mRNA into fertilized eggs of *H. pulcherrimus*, and genomic DNA was extracted at 24 hpf from 20 embryos injected with SpCas9/sgRNA or SpCas9 alone. CRISPR-Cas9-mediated mutagenesis was examined by HMA. In the PCR product from embryos injected with SpCas9 alone (control), a clear and distinct band of the expected size was detected for each target site (Figure 5b, c). When sgRNA#1, which corresponds to Sp.PKS1.175(+), was microinjected, no band shift was detected (Figure 5b). However, the PCR products from embryos injected with either sgRNA#2, corresponding to Sp.PKS1.547(−), or sgRNA#3, corresponding to Sp.PKS1.806(−), produced shifted bands, representing heteroduplexes formed by mutated alleles (Figure 5c), indicating that injection of either sgRNA#2 or sgRNA#3 introduced mutations at the target site within *HpPks1*.

To examine the timing of SpCas9/sgRNA-mediated mutagenesis during sea urchin embryogenesis, HMA was performed at different time points after fertilization using SpCas9/sgRNA#2-injected embryos. The band shift was not detected at 4 hpf and was first detected at 8 hpf in SpCas9/sgRNA#2-injected embryos. The intensity of the shifted band increased to a maximum at 12 hpf (Figure 5d). Furthermore, in a detailed analysis, the shifted band representing the mutagenesis was first detected at 6 hpf in SpCas9/sgRNA#2-injected embryos (data not shown). These results suggested that the CRISPR-Cas9-induced mutations were introduced during the early stages of development (morula to early blastula stages) in *H. pulcherrimus*.

To analyze the types and efficiency of mutations induced by CRISPR-Cas9-mediated genome editing, the PCR amplicons were subcloned and sequenced. Among 17 sequenced clones from sgRNA#2-injected embryos, deletions (15 clones) and deletion/insertion (two clones) were observed, and thus, the mutation rate was 100% (Figure 7a). However, as many clones showed deletions of three or multiples of three nucleotides, the frameshift rate was 17.6%. On the other hand, among 15 sequenced clones from sgRNA#3-injected embryos, deletion (seven clones), substitution (one clone), insertion (one clone), and deletion/insertion (three clones) were observed (Figure

7b), indicating a mutation rate of 80%, with 40% being frameshift mutations. Furthermore, deletions seemed to be caused not only by NHEJ, but also by MMEJ (Figure 7, underline).

Off-target analysis in *HpPks1* sgRNA-injected embryos

As programmable nucleases used in genome editing can induce undesirable off-target effects, I assessed off-target effects in CRISPR-Cas9-mediated mutagenesis targeting the *HpPks1* gene in *H. pulcherrimus*. To find potential off-target sites for sgRNA#2 and #3, I searched for homologous sequences of the sgRNA target sites in *H. pulcherrimus* genome in *HpBase*. I did not identify any homologous sequence of the sgRNA#3 target site. However, potential off-target sites for sgRNA#2 were detected, and four of them (in scaffolds 68, 1135, 5844, and 13705) showed sequence identity in the PAM sequence and 12 nucleotides 3′ of the PAM sequence (Figure 8a). Previous studies have shown that a 12-nucleotide seed region of a sgRNA adjacent to the PAM site is more important than the rest of the target sequence for specific binding (Jiang et al., 2013; Larson et al., 2013). I carried out HMA and sequencing analyses for two of these potential off-target sites; I did not detect any mutations in these potential off-target sites (Figure 8b, c), suggesting that CRISPR-Cas9-mediated mutagenesis targeting *HpPks1* in this study was highly specific to the target site.

Albino phenotype in *HpPks1* sgRNA-injected larvae

I analyzed the phenotype of the sgRNA-injected embryos. All of the control embryos injected with SpCas9 mRNA alone developed normally (Figure 9a). The sgRNA#1-injected embryos also developed normally and were morphologically indistinguishable from control embryos (data not shown). However, when either sgRNA#2 or sgRNA#3 was injected, pigment deficiency was observed in larvae in the pluteus stage (Figure 9b–d). All of the sgRNA#2-injected pluteus larvae exhibited complete loss of pigment (Figure 9b, e). On the other hand, 28% of sgRNA#3-injected larvae exhibited complete

loss of pigment (Figure 9c, e) and 60% exhibited partial loss of pigment (Figure 9d, e). These results indicated that the *HpPks1* gene was disrupted in the SpCas9/sgRNA-injected embryos and that gene knockout by the introduction of sgRNA#2 and sgRNA#3 resulted in pigment deficiency.

Effect of *HpPks1* knockout in late pluteus larvae and adult sea urchins

To gain insights into the effects of CRISPR-Cas9-mediated knockout on late developmental processes of *H. pulcherrimus* and to establish knockout adult sea urchin, control and SpCas9/sgRNA-injected larvae were further cultured by feeding them the microalgae *C. gracilis*. The sgRNA#2 or sgRNA#3-injected larvae grew normally and their albino phenotype was maintained during late larval development (Figure 10a–c). Adult rudiment was normally formed on the left side of the larval body (Figure 10d–f) and grew similarly as in the control (Figure 10g–i). In addition, sgRNA-injected larvae showed pigment deficiency not only in the larval body, but also in the adult rudiment. After metamorphosis, sgRNA-injected juvenile sea urchin also exhibited pigment deficiency (Figure 10k, l). In control juvenile sea urchin, pigmentation was normal (Figure 10j). We further monitored the growth of control and sgRNA#2-injected knockout individuals (Figure 11). Whereas 3-month-old adult control sea urchins showed an obvious five-fold symmetric pigmentation pattern, *HpPks1*-knockout adult sea urchins showed an albino phenotype (Figure 11a, b). Both control and *HpPks1*-knockout individuals grew normally to adulthood, but the *HpPks1*-knockout individuals did not exhibit pigmentation on the surface, spines, and tube feet (Figure 11c–f). *HpPks1*-knockout urchins survived until 1 year of age and grew to more than 1 cm in diameter, and 1-year-old *HpPks1*-knockout individuals still showed the albino phenotype (Figure 11g, h). Skeletons of *HpPks1*-knockout adult sea urchins also showed pigment deficiency (Figure 11i, j), suggesting that sgRNA#2-mediated knockout was effective in the entire body.

To analyze genotypic variation in individual adult sea urchins, genomic DNA was extracted from three control and three *HpPks1*-knockout sea urchins of 5 months old.

HMA and sequencing analyses revealed that *HpPks1*-knockout individuals lacked the wild-type allele, whereas each *HpPks1*-knockout individual had various types of mutations (Figure 12). These results indicated that *HpPks1*-knockout adult sea urchins were successfully established.

Effect of *HpPks1* knockout in the expression of other pigment cell related gene

The specification of the pigment cell is initiated by the activation of the gene encoding the transcription factor Gcm by Delta signaling received from the skeletogenic mesoderm (Materna et al., 2013; Ransick & Davidson, 2006; Croce & McClay, 2010; Peterson & McClay, 2005). To explore the effect of *HpPks1* knockout on the expression of *HpPks1* and *HpGcm* genes, the expressions of *HpPks1* and *HpGcm* mRNAs was examined by WMISH. Approximately two third of sgRNA#2-injected embryos showed *HpPks1* mRNA expression in the secondary mesenchyme cells (Figure 13a, b), suggesting that this *HpPks1* knockout does not disrupt its own transcription. Furthermore, the expression of *HpGcm* had no difference between control and sgRNA#2-injected embryos (Figure 13c, d) indicating that the disruption of *HpPks1* function has effect only on the pigmentation, but not on the differentiation of secondary mesenchyme cells and pigment cells.

Discussion

In this thesis, I confirmed that CRISPR-Cas9 system can be used for targeted mutagenesis in *H. pulcherrimus*. I successfully disrupted the *HpNodal* gene in the sea urchin embryo using the CRISPR-Cas9 system. Introduction of sgRNA#1 targeting *HpNodal* gene achieved 65% of mutagenesis efficiency and embryos showed abnormal of skeletogenesis and radialized shape, which is comparable to the preceding study using *S. purpuratus* (Lin & Su, 2016).

I successfully disrupted the *HpPks1* gene in the sea urchin *H. pulcherrimus* using the CRISPR-Cas9 system and established knockout adult sea urchin. The albino phenotype was maintained in *HpPks1*-knockout adult sea urchin, suggesting that *Pks1* is required for pigmentation not only in pluteus larvae, but also in adult sea urchin, and that polyketide compounds are involved in the colorful pigmentation of adult sea urchins.

The preceding study using *S. purpuratus* introduced a combination of three sgRNAs targeting the Pks1 gene and resulted in efficient mutagenesis and larval albino phenotype, but only a slight portion of embryos showed pigmentation (Oulhen & Wessel, 2016). A similar albino phenotype was reported using CRISPR-Cas9 and CRISPR-Cas9-deaminase by introduction of mixture of 16 sgRNAs targeting the *Pks1* gene, but the efficiency was not so high (Shevidi et al., 2017). Whereas, in this study, I introduced single sgRNA, and the introduction of sgRNA#2 achieved 100% of mutagenesis efficiency and all injected embryos showed the complete loss of pigmentation. I speculate that mixing multiple sgRNA may result in dilution of the effect of highly efficient sgRNA and may increase the rate of undesirable effects, such as off-target effects. Therefore, usage of single highly efficient sgRNA may be desirable for efficient genome editing.

In previous studies, the knockout rates achieved with ZFN- and TALEN-mediated genome editings were 9.5% and 12.6%, respectively (Hosoi et al., 2014; Ochiai et al., 2010). Although the efficiencies cannot be simply compared because different target loci were used, the knockout efficiency of the CRISPR-Cas9 was much higher than those of

ZFN and TALEN in *H. pulcherrimus.* CRISPR-Cas9-mediated mutagenesis by sgRNA#2 targeting *HpPks1* achieved a mutation rate of 100%, with all Cas9/sgRNA-injected embryos exhibiting the albino phenotype, suggesting that the CRISPR-Cas9 system can efficiently induce biallelic genome modifications in *H. pulcherrimus* embryos. Although the mutation rate of sRNA#2 was 100%, many alleles showed deletions of three or multiples of three nucleotides, and the frameshift rate was 17.6%. Nonetheless, all SpCas9/sgRNA-injected embryos showed the albino phenotype, indicating that the essential residue for HpPKS1 enzymatic function is located in the sRNA#2-targeted site. In other words, it is important to target the gene sequence encoding an essential residue, although the requirement of a PAM sequence may be a restriction for target sequence design in the CRISPR-Cas9 system.

Mutations introduced by ZFN were weakly detected at 4 hpf and TALEN-mediated mutagenesis was not observed until 8 hpf (Hosoi et al., 2014; Ochiai et al., 2010). In this study, CRISPR-Cas9-mediated mutagenesis was detected as of 6 hpf. Therefore, the timing of CRISPR-Cas9 mediated genome editing is comparable to those of ZFN and TALEN. Ribonucleoprotein (RNP) consisting of the SpCas9 protein in complex with sgRNA has been used in cultured cells and animals (Kim et al., 2014; Kotani et al., 2015; Lee et al., 2014; Sakane et al., 2018; Shigeta et al., 2016; Sung et al., 2014); it shortens the timing of genome editing and overcomes the mosaic property (Kim et al., 2014; Kotani et al., 2015). I attempted to accelerate mutagenesis in *H. pulcherrimus* by using SpCas9 RNP. However, upon microinjection of SpCas9 RNP, I did not observe mutations in *H. pulcherrimus* (Figure 14). Although this may be because of the experimental conditions used, such as the concentration of SpCas9 protein and the ratio between SpCas9 protein and sgRNA, this may suggest that SpCas9 RNP may not be feasible for CRISPR-Cas9-me-diated mutagenesis in sea urchin.

Off-target effects are a critical concern for genome editing tools. A mismatch in the seed sequence (12 nucleotides adjacent to the PAM sequence) disrupts target specificity, and SpCas9 tolerates single-base mismatches in the PAM-distal region to a greater extent than in the PAM-proximal region (Cong et al., 2013; Hsu et al., 2013). Furthermore, up to six contiguous mismatches in the 5′-terminal region of the protospacer are tolerated

(Jinek et al., 2012), and CRISPR-Cas9 can induce mutations at off-target sites with up to five mismatches (Fu et al., 2013). By screening the *H. pulcherrimus* genome, I found four potential off-target sites of sgRNA#2 that showed sequence identity in the PAM sequence and 12 nucleotides 3′ of the PAM. Scaffold 68 (OT1) and scaffold 1135 (OT2) have six and five mismatches, respectively. However, HMA and sequencing analysis did not reveal any mutations induced by sgRNA#2 at these potential off-target sites (Figure 8b, c). A previous study showed that the maximum detection limit of HMA for CRISPR-Cas9-mediated mutant alleles was 0.5% in mouse pups and human cultured cells (Zhu et al., 2014). Although nucleotide variations were detected by sequencing, they are probably polymorphisms as they were positioned at a distance from the potential off-target sites and the sea urchin genome is highly polymorphic (Britten et al., 1978; Sea Urchin Genome Sequencing Consortium, 2006; Yamamoto et al., 2007). These findings suggest that sgRNA#2 is highly specific to *HpPks1* and produces no detectable off-target effect.

During sea urchin larval development, the adult rudiment develops from left side of the coelomic pouch, which originates from small micromere and macromere descendants (Cameron et al., 1987; Cameron et al., 1991). The amniotic invagination of the ectoderm merges with the coelomic pouches to form an adult rudiment (Smith et al., 2008). Consistent with the multiple cell lineages of the adult rudiment, F0 knockout adult sea urchins exhibited multiple genotypes even after metamorphosis (Figure 12). Therefore, to obtain adult sea urchins of a single knockout genotype, an F1 generation should be generated. Although relatively large deletions (29, 37 and 48 bps) were observed in the adult knockout sea urchins (Figure 12) compared with those in the knockout embryos (Figure 7). However, this difference is probably due to the variation between experimental batch because the same batch of *Pks1* knockout embryos also showed large deletion (Figure 12).

In conclusion, I showed that the CRISPR-Cas9 system is a highly effective tool for genome editing in *H. pulcherrimus*. I successfully established not only knockout embryos, but also knockout adult sea urchins with an albino phenotype. Therefore, the CRISPR-Cas9 system can be used for the analysis of late developmental processes, such

as the formation of adult rudiment, establishment of the five-fold symmetry of the adult body plan, and the mechanism of metamorphosis. Furthermore, albino adult sea urchins may be useful for the analysis of cell lineages and gene expression by use of fluorescent proteins during the morphogenesis of adult tissues.

Figures

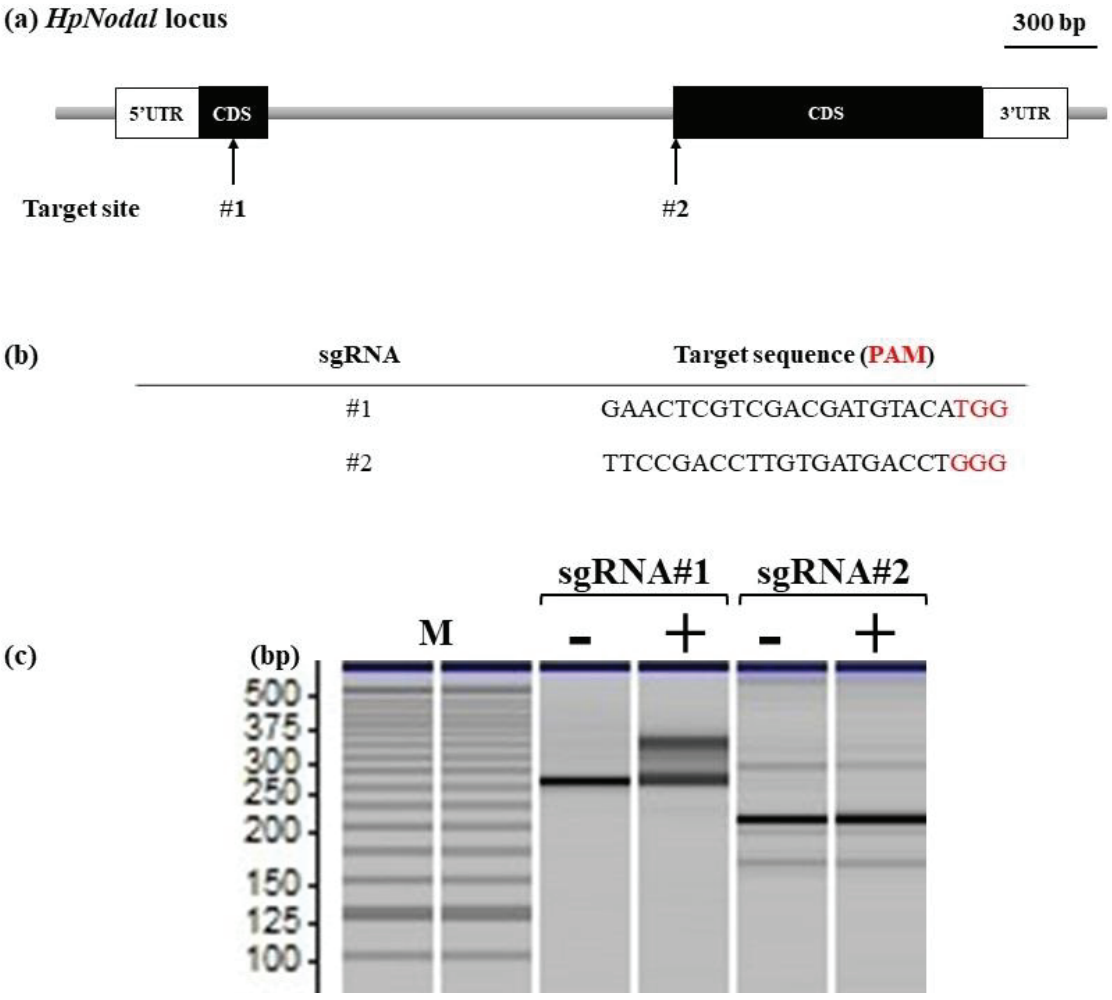

Figure 1 CRISPR-Cas9-mediated mutagenesis of the *HpNodal* gene. (a) Schematic illustration of the *HpNodal* gene. The two exons are indicated by black boxes. The arrows indicate the target sites used in this study. (b) Target sequence of sgRNAs, PAM sequence is marked in red. M: DNA ladder. (c) Genotyping of sgRNA-injected embryos by HMA. Genomic DNA was extracted from 20 embryos injected with SpCas9 alone (−) or SpCas9/sgRNA (+) at 24 hpf, and the target site was analyzed by HMA using MultiNA.

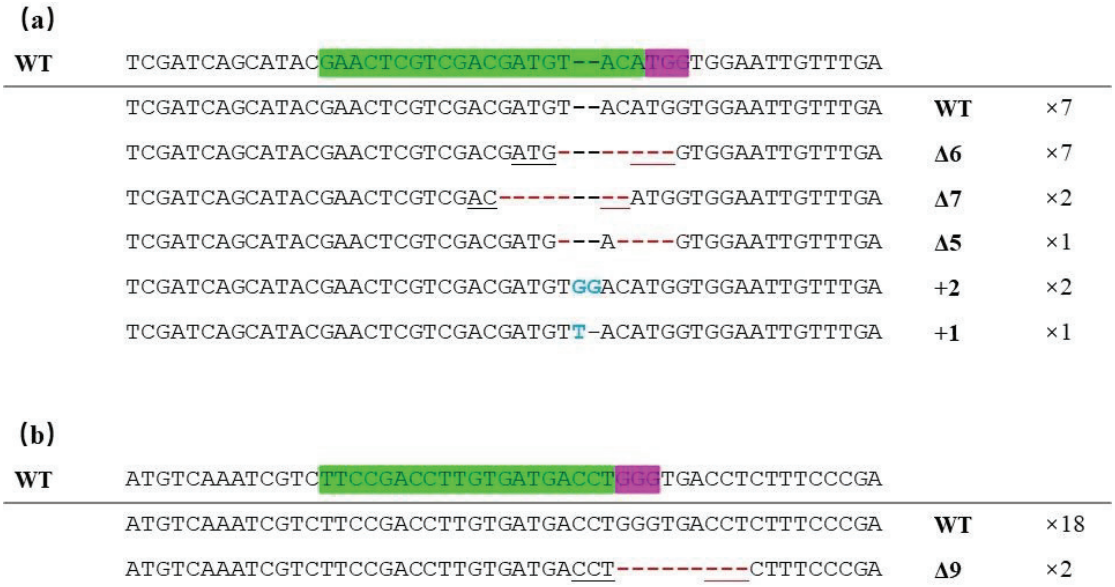

Figure 2 Sequence analysis of mutations induced by sgRNA#1 and sgRNA#2. (a) Mutations observed in sea urchin embryos injected with sgRNA#1. (b) Mutations observed in sea urchin embryos injected with sgRNA#2. The wild-type sequences are shown on the top, with the PAM highlighted in magenta and the protospacer highlighted in green. Deletions, substitutions, and insertions are indicated by red dashes, red letters, and blue letters, respectively. Microhomologous sequences are underlined.

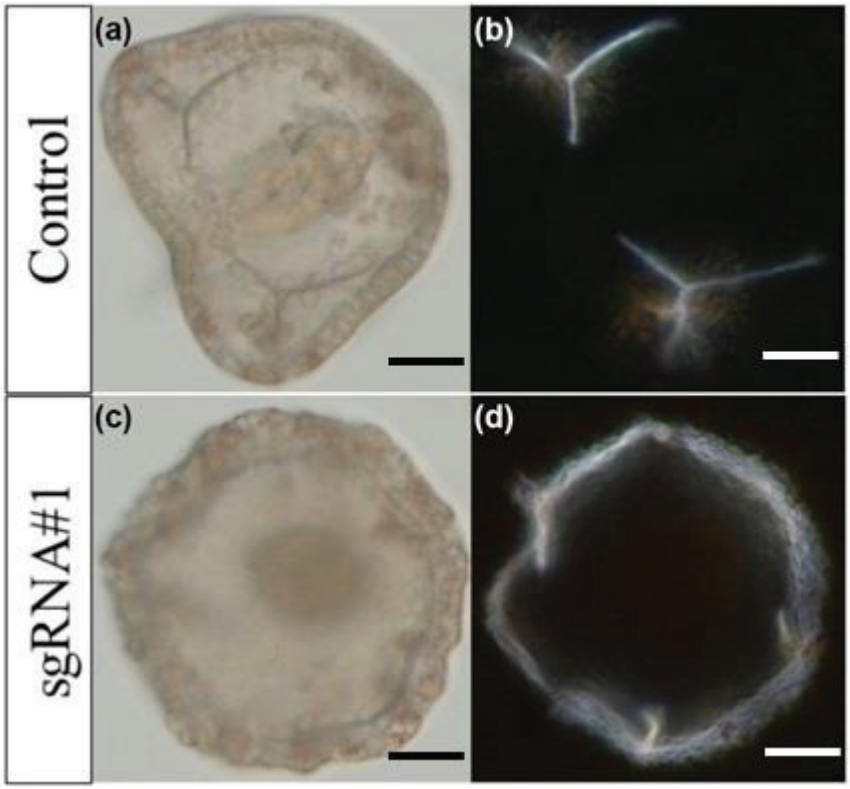

Figure 3 Phenotypes of *HpNodal*-targeted larvae. (a, b) Control embryo. (c, d) sgRNA#1-injected embryo showing abnormal of skeletogenesis. (a, c) Bright-field images of embryos. (b, d) Polarized microscopic images of embryos. Scare bar: 50 μm.

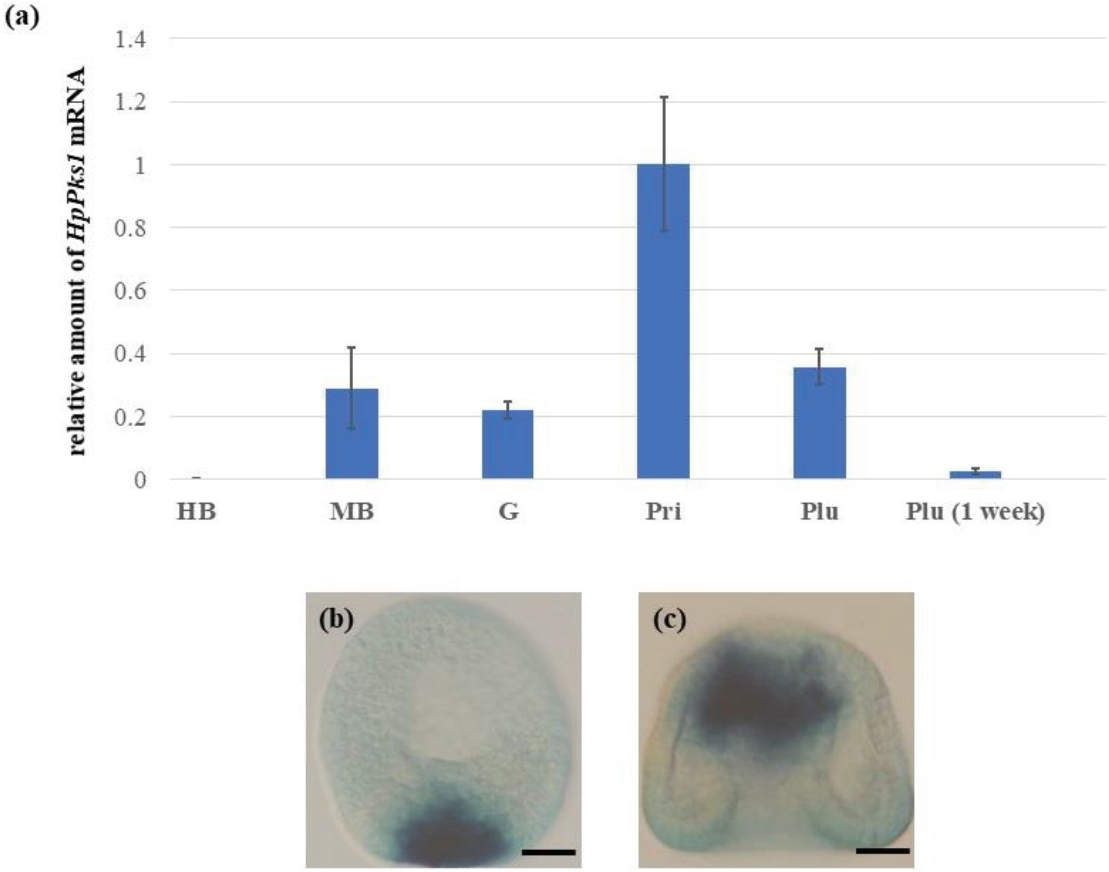

Figure 4 Temporal and spatial expression of *HpPks1* in early development of *H. pulcherrimus*. (a) qRT-PCR analysis of *HpPks1* mRNA expression. HB: Hatched blastula; MB: Mesenchyme blastula; G: Gastrula; Pri: Prism; Plu: Pluteus. (b, c) WMISH showing the spatial expression of *HpPks1*. (b) Mesenchyme blastula; (c) Gastrula. Scare bar: 50 μm.

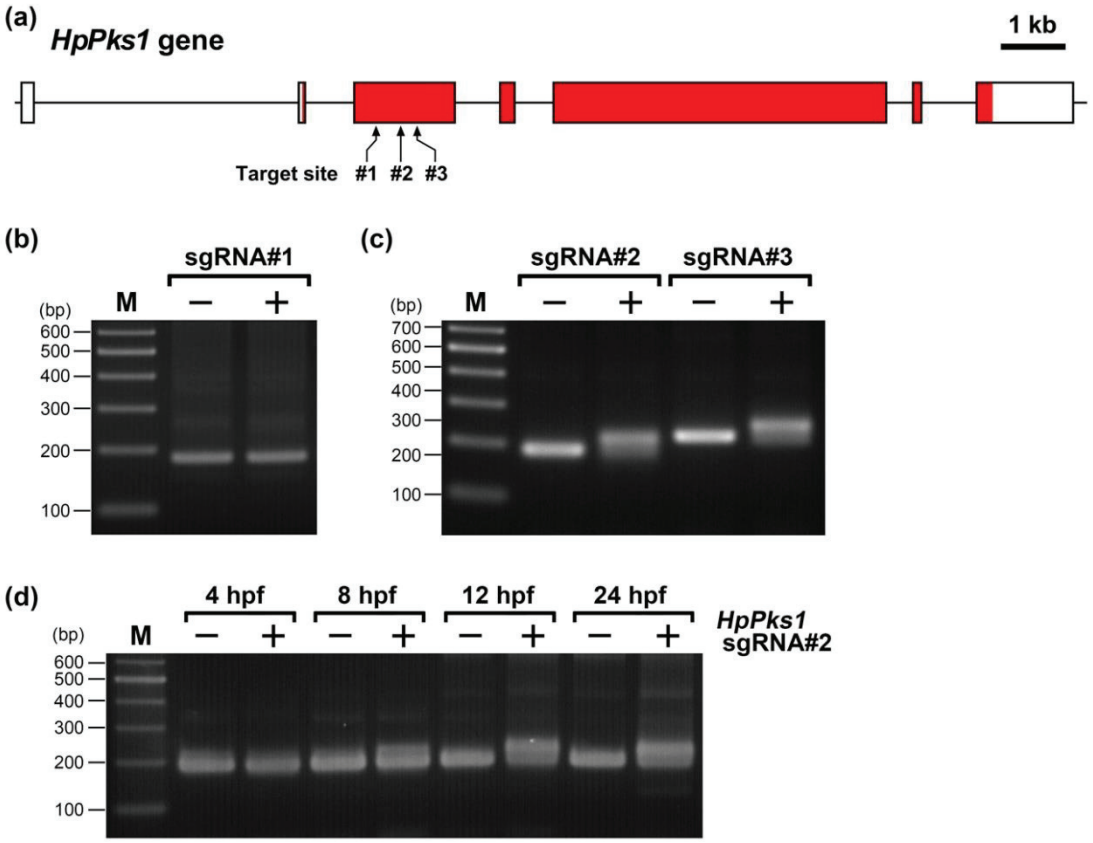

Figure 5 CRISPR-Cas9-mediated mutagenesis of the *HpPks1* gene. (a) Schematic illustration of the HpPks1 gene. The exons are indicated by boxes, and coding regions are indicated in red. The arrows indicate the target sites used in this study. (b) Genotyping of sgRNA#1-injected embryos by HMA. Genomic DNA was extracted from 20 embryos injected with SpCas9 alone (−) or SpCas9/sgRNA#1 (+) at 24 hpf, and the target site #1 was analyzed by HMA. (c) Genotyping of sgRNA#2 or sgRNA#3-injected embryos by HMA. Genomic DNA extracted from 20 embryos at 24 hpf was analyzed by HMA. (d) Examination of the timing of CRISPR-Cas9-mediated mutagenesis. Genomic DNA was extracted 20 embryos injected with SpCas9 alone (−) or SpCas9/sgRNA#2 (+) at 4, 8, 12, and 24 hpf, and used for HMA. PCR products were separated using 3% agarose gel electrophoresis. M: 100-bp DNA ladder.

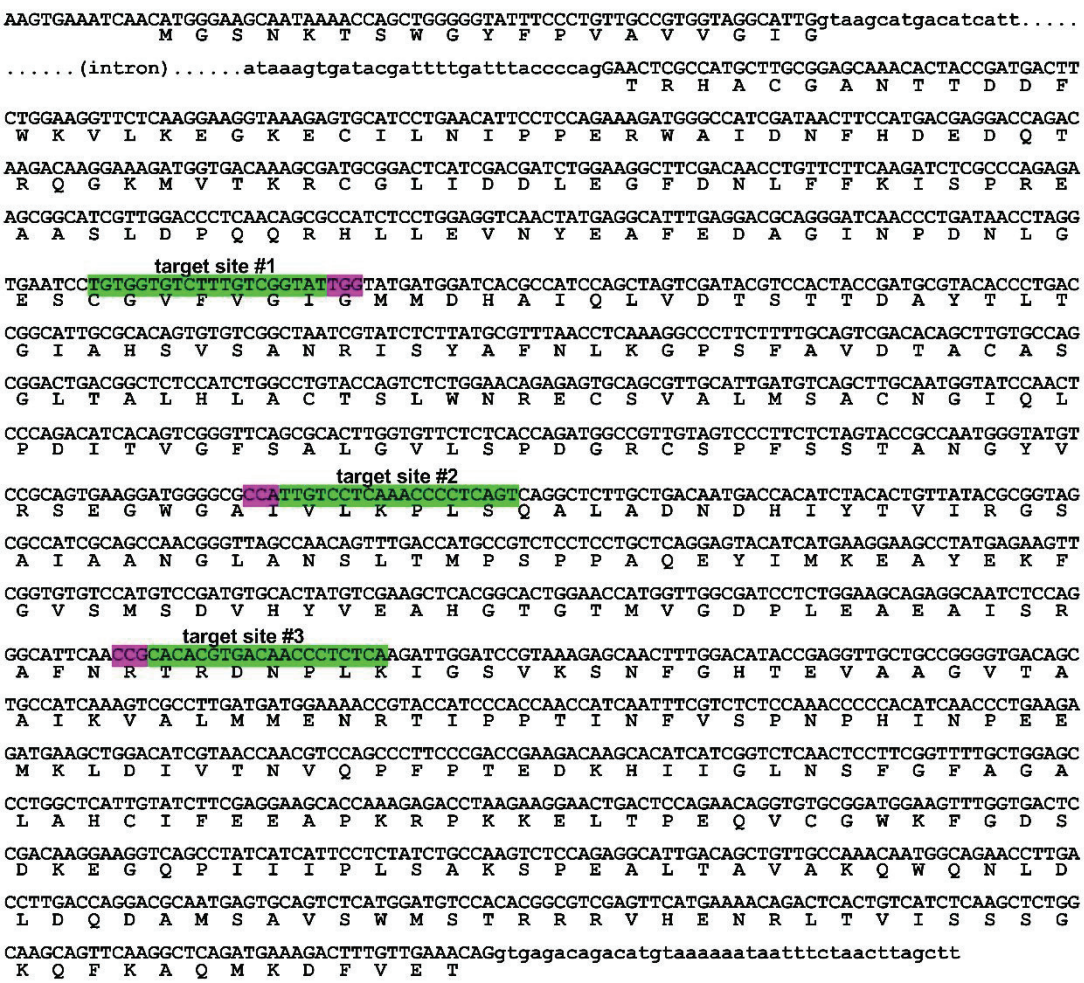

Figure 6 Nucleotide sequence of the target region in the *HpPks1* gene. Capitalized letters represent the exon, and lower-case letters represent introns. Target sites and PAM are highlighted in green and magenta, respectively.

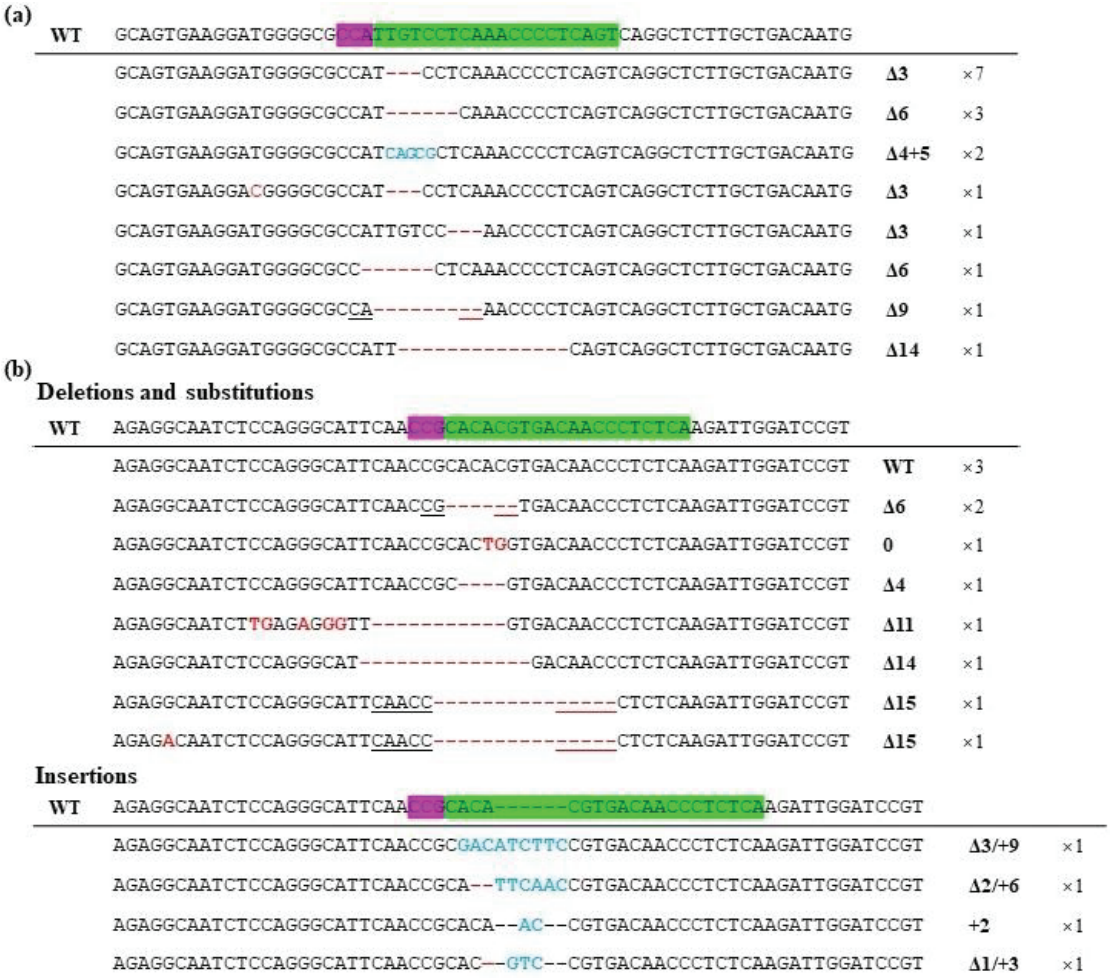

Figure 7 Sequence analysis of mutations induced by sgRNA#2 and sgRNA#3. (a) Mutations observed in sea urchin embryos injected with sgRNA#2. (b) Mutations observed in sea urchin embryos injected with sgRNA#3. The wild-type sequences are shown on the top, with the PAM highlighted in magenta and the protospacer highlighted in green. Deletions, substitutions, and insertions are indicated by red dashes, red letters, and blue letters, respectively. Microhomologous sequences are underlined.

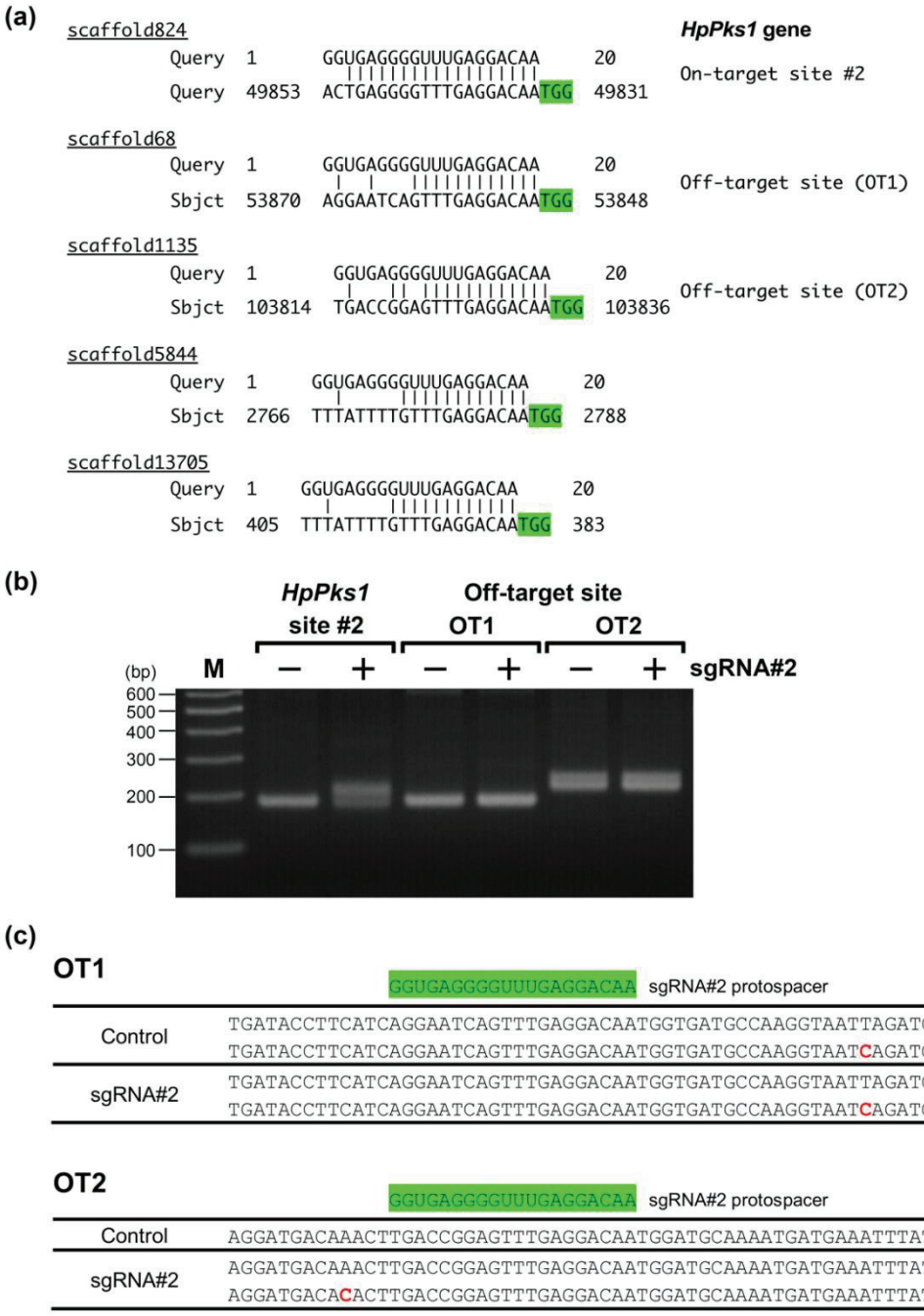

Figure 8 Potential off-target sites for sgRNA#2. (a) Comparison of nucleotide sequences between sgRNA#2 protospacer and putative off-target sites. Vertical lines indicate identical nucleotides. Possible PAM sequences are highlighted in green. (b) HMA of potential off-target sites OT1 and OT2. Genomic DNA was extracted from 20 embryos injected with SpCas9 alone (−) or SpCas9/sgRNA#2 (+) at 24 hpf, and the target site #2 and off-target sites (OT1 and OT2) were analyzed by HMA. PCR products were separated using 3% agarose gel electrophoresis. (c) Sequence analysis of OT1 and OT2. Nucleotide variations are indicated by red letters.

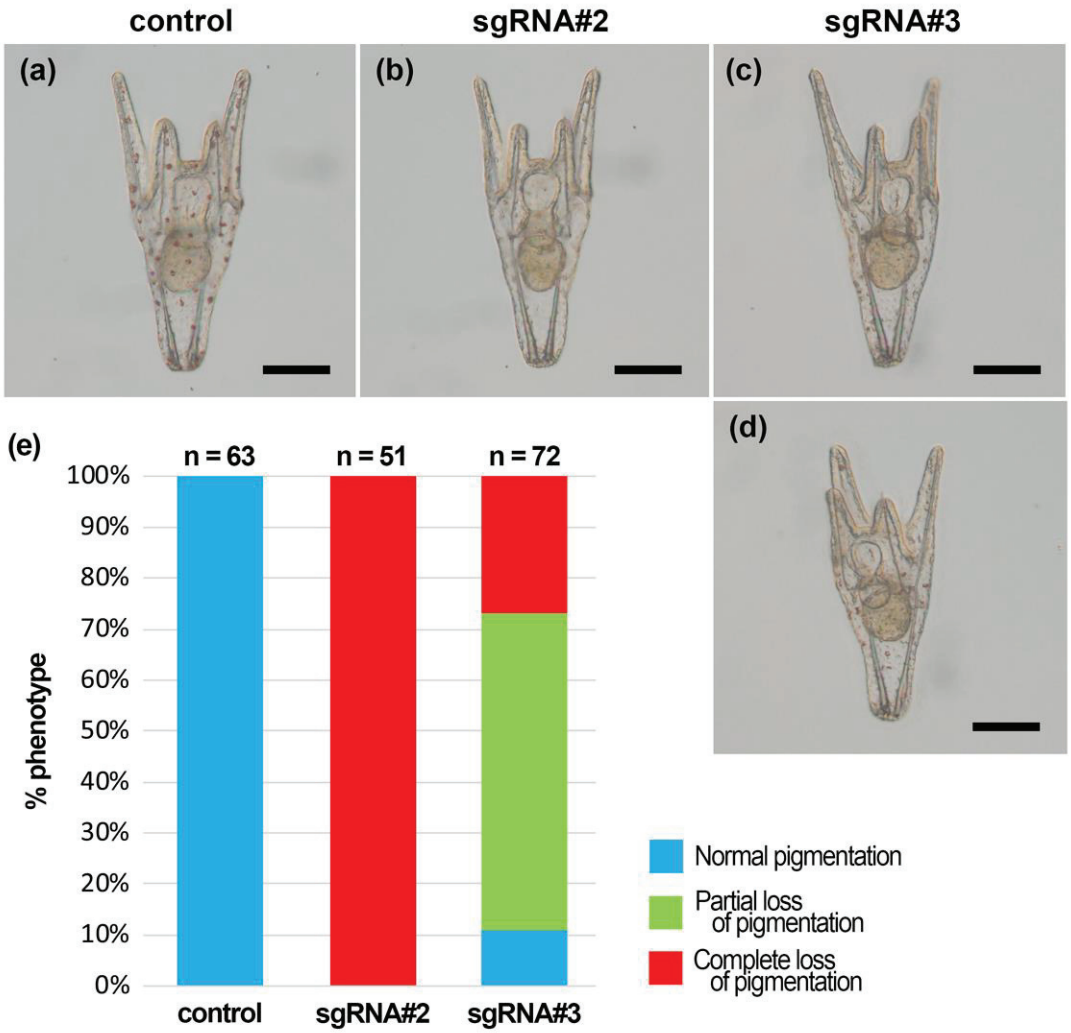

Figure 9 Phenotypes of *HpPks1*-targeted larvae. (a–d) Representative images of larvae injected with SpCas9 alone (a), SpCas9/sgRNA#2 (b), and SpCas9/sgRNA#3 (c, d). Scale bars: 100 μm. (e) The phenotype frequencies are shown in the graph. Phenotypes were classified into three groups: normal pigmentation, partial loss of pigmentation, and complete loss of pigmentation. Total numbers of larvae are shown at the top of each bar.

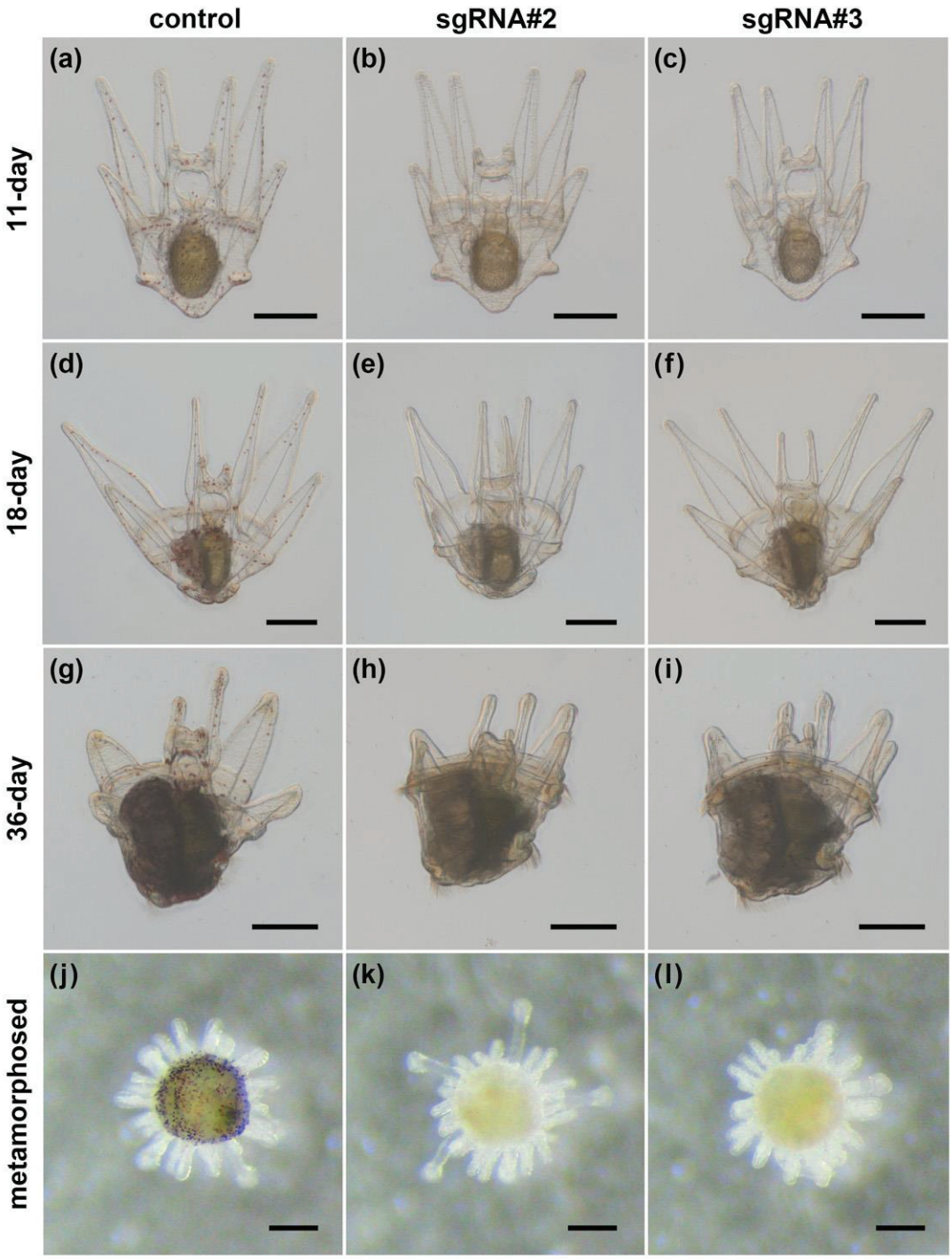

Figure 10 Albino phenotype observed during larval stages and after metamorphosis. (a–c) Eleven-day larvae. (d–f) Eighteen-day larvae. (g–i) Thirty-six-day larvae. (j–l) Juvenile sea urchins at 1 day after metamorphosis. Representative images of control larvae injected with SpCas9 alone (a, d, g), control juvenile sea urchin injected with SpCas9 alone (j), sgRNA#2-injected larvae (b, e, h), sgRNA#2-injected juvenile sea urchin (k), sgRNA#3-injected larvae (c, f, i) and sgRNA#3-injected juvenile sea urchin (l) are shown. Scale bars: 200 μm.

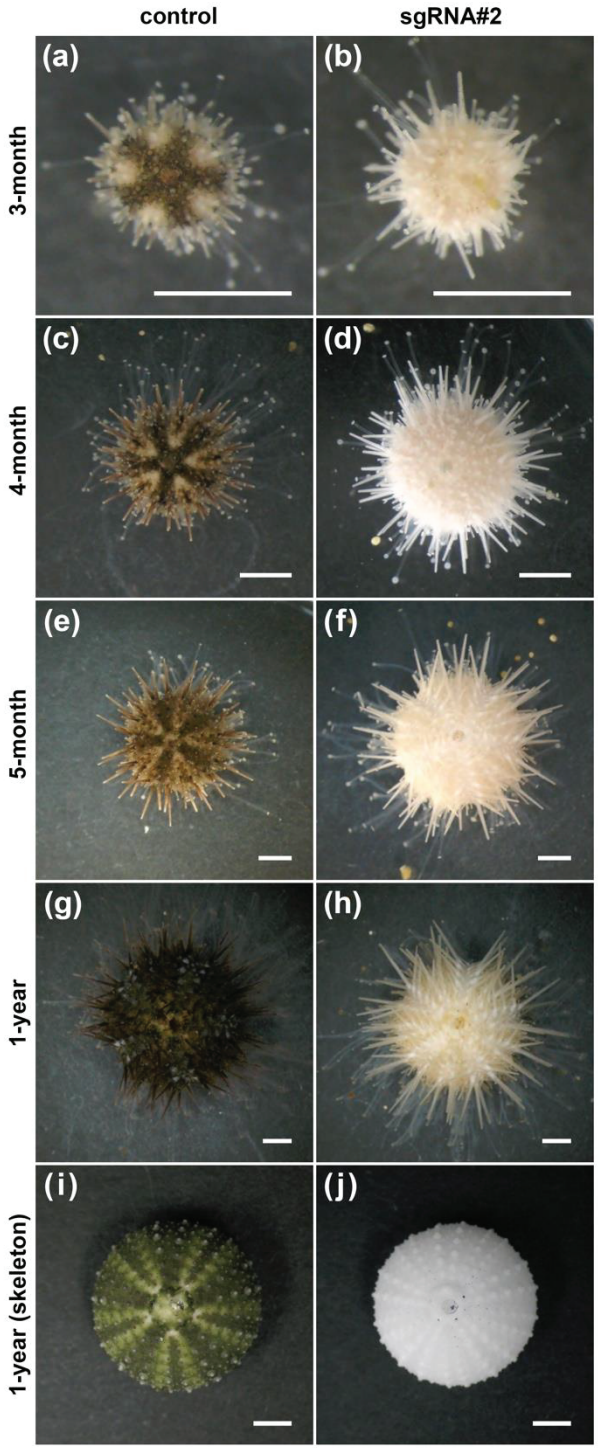

Figure 11 Albino phenotype observed in adult sea urchins. (a, b) Adult sea urchin of 3 months. (c, d) Adult sea urchin of 4 months. (e, f) Adult sea urchin of 5 months. (g, h) Adult sea urchin of 1 year. (i, j) Skeletons of adult sea urchin of 1 year. Representative images of control sea urchin injected with Cas9 alone (a, c, e, g, i) and sgRNA#2-injected sea urchins (b, d, f, h, j) are shown. Scale bars: 2 mm

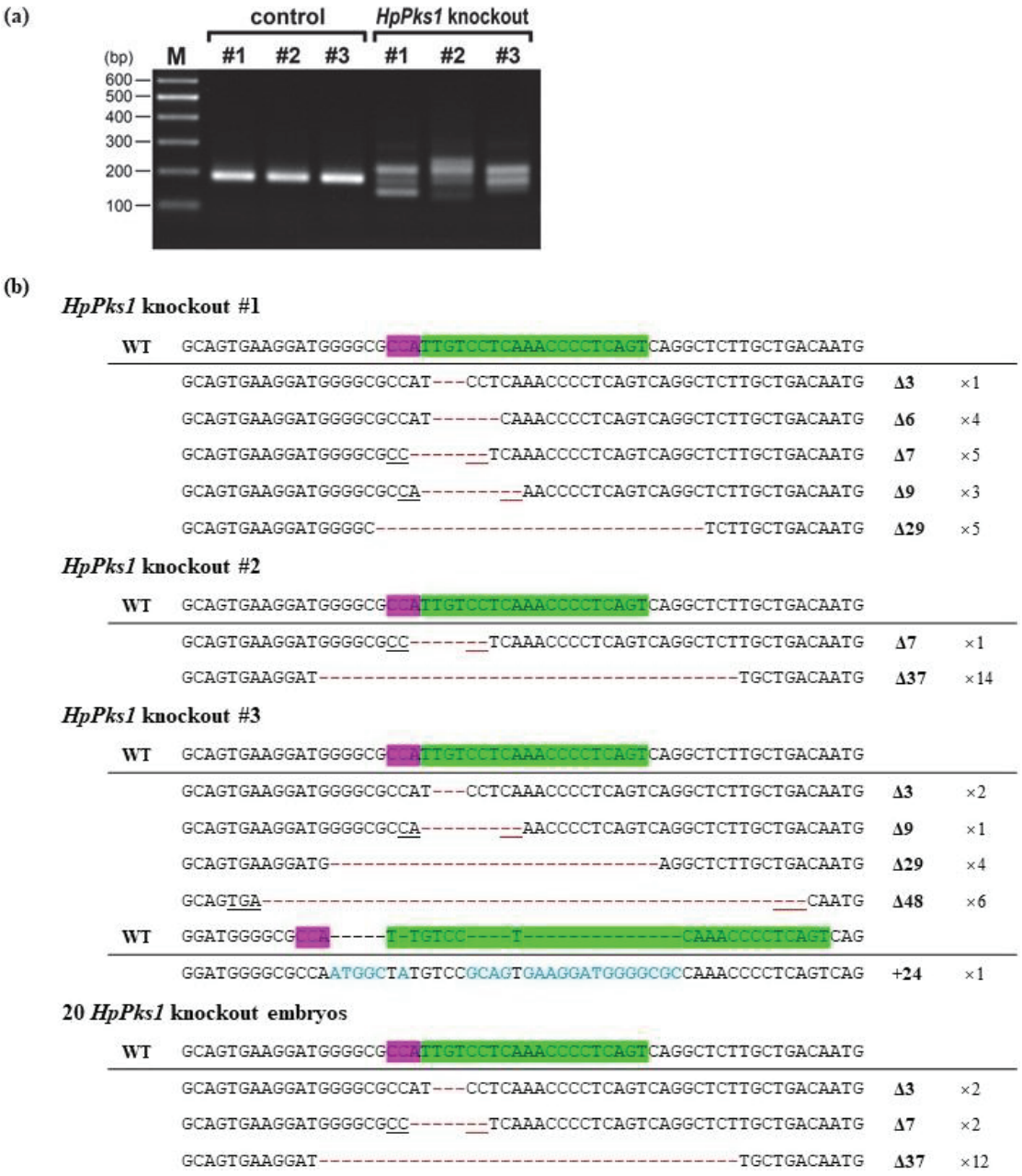

Figure 12 Genotyping of individual sea urchins injected with SpCas9 alone and SpCas9/sgRNA#2. (a) Genotyping by HMA. Genomic DNA was extracted from 5-month-old individual sea urchins injected with SpCas9 alone (control) or SpCas9/sgRNA#2 (*HpPks1* knockout), and the target site #2 was analyzed by HMA. PCR products were separated on a 0.5% agarose gel supplemented with resolution enhancer. M: 100-bp DNA ladder. (b) Sequences observed in three individual *HpPks1*-knockout adult sea urchins and 20 *HpPks1*-knockout embryos. The wild-type sequences are shown on top with the PAM highlighted in magenta and the protospacer highlighted in green. Deletions, substitutions, and insertions are indicated by red dashes, red letters, and blue letters, respectively. Microhomologous sequences are underlined.

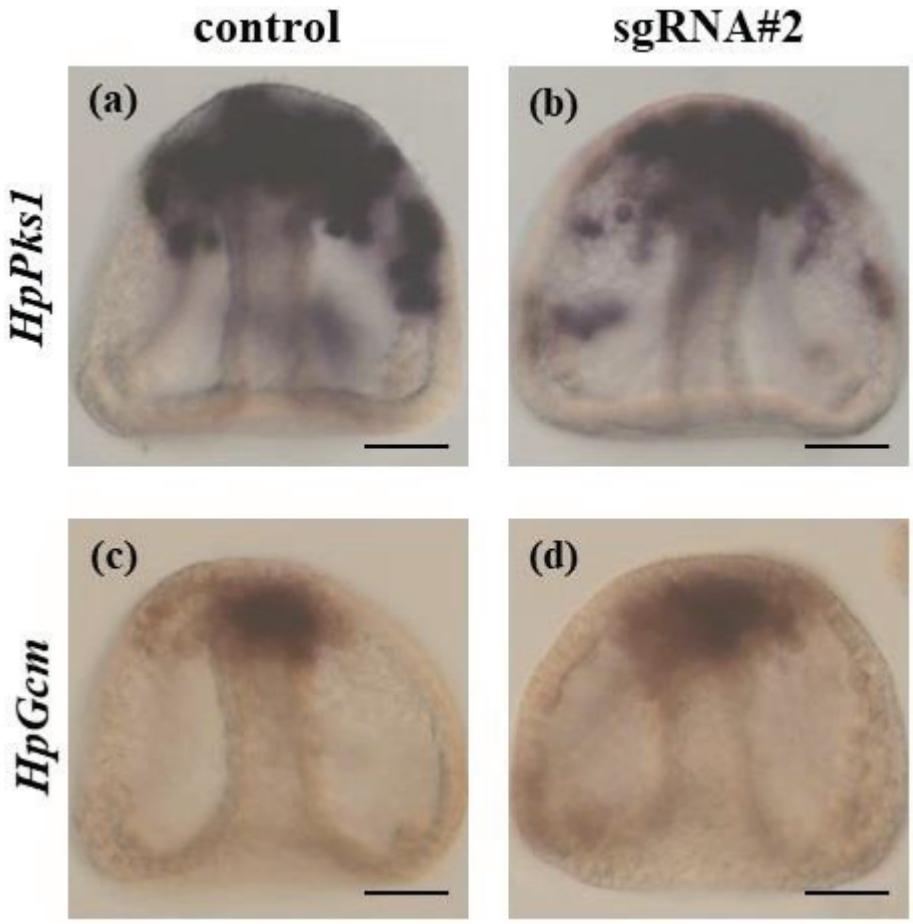

Figure 13 WMISH showing the spatial expression of *HpPks1* and *HpGcm* at 28 hpf. (a, b) Spatial expression of *HpPks1*. (c, d) Spatial expression of *HpGcm*. Representative images of control sea urchin embryos injected with SpCas9 alone (a, c) and SpCas9/sgRNA#2-injected embryos (b, d) are shown. Scale bars: 50 μm.

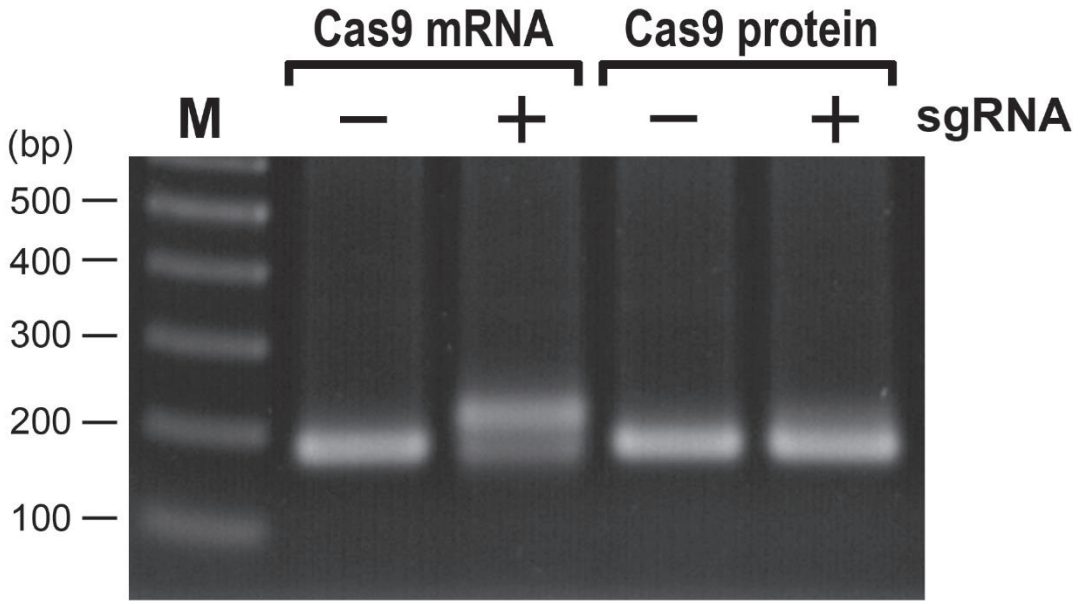

Figure 14 Genotyping by HMA in Cas9 RNP-injected embryos. Cas9 mRNA (750 ng/ul) or recombinant Cas9 protein (750 ng/ul; Alt-R S.p. Cas9 Nuclease 3NLS; integrated DNA Technologies, IA,USA) was used for microinjection in the presence (+) or absence (-) of 150 ng/ul of sgRNA#2. Genomic DNA was extracted from 20 injected embryos at 24 hpf, and the sgRNA#2 target site was analyzed by HMA. Distinct shifted bands were not detected in the analysis of Cas9 RNP-injected embryos. PCR products were separated on a 0.5% agarose gel supplemented with resolution enhancer. M: 100-bp DNA ladder.

Table 1. Oligonucleotides used for sgRNA synthesis

name	nucleotide sequence (5' to 3')
Nodal #1-fwd	GTAATACGACTCACTATATGTACATCGTCGACGAGTCCGTTTTAGAGCTAGAAATAG
Nodal #2-fwd	GTAATACGACTCACTATAAGGTCATCACAAGGTCGGCCGTTTTAGAGCTAGAAATAG
Pks1 #1-fwd	GTAATACGACTCACTATAGGTGGTGTCTTTGTCGGTATGTTTTAGAGCTAGAAATAG
Pks1 #2-fwd	GTAATACGACTCACTATAACTGAGGGGTTTGAGGACAAGTTTTAGAGCTAGAAATAG
Pks1 #3-fwd	GTAATACGACTCACTATATGAGAGGGTTGTCACGTGTGGTTTTAGAGCTAGAAATAG
Reverse-sgRNA	TCGGTGCCACTTTTTCAAGTTGATAACGGACTAGCCTTATTTTAACTTGCTATTTCTAGCTCTAAAAC
T7-sgRNA-fwd	CAGTGAATTGTAATACGACTCACTATAG
sgRNA-rev	AAAAAAGCACCGACTCGGTGCCACTTTTTCAAG

Table 2. Primers used in this study.

Target site	Forward primer sequence (5' to 3')	Reverse primer sequence (5' to 3')
Nodal #1	CGGCTGTCGTCTGCTTATTT	CCTTGGATGGGTTGACAAGA
Nodal #2	AATCGTCTTCCGACCTTGTG	ATCAGCTTGCGTTGCTGAC
Pks1 #1	AACAGCGCCATCTCCTGGAGGTCAAC	TTAGCCGACACACTGTGCGCAATGCC
Pks1 #2	GCACTTGGTGTTCTCTCACCAGATGG	GGTCAAACTGTTGGCTAACCCGTTGG
Pks1 #3	TGAGAAGTTCGGTGTGTCCATGTCCG	GTACGGTTTTCCATCATCAAGGCGAC
OT1	AGCCTGTGTTGAGCAAGATCGTGAGG	CACCTTTGTCTTCTCCTACCTGTGGG
OT2	GAAGGAGTGACGAATTTGAATGACGC	TCCTGGAATCTTATCTTCAGCATCTC
Pks1 WMISH	AACAGTTTGACCATGCCGTC	TCATCTGAGCCTTGAACTGC
Gcm WMISH	ACTCACTTCAACGCCTCACA	ACACATGCGCTCCTCTTTCA
Pks1 qPCR	ACCTGACGGAAAGCGGAAAA	TCTTTGCAATCCCACCGTCT
Gcm qPCR	AAATCGTGACTGTTCGGCCA	CAAAAGTGCGTTACAGGGTAGC
MitCOI qPCR	GGCACAGCTATGAGTGTAATTATCC	GATAGTTCATCCAGTCCCTGCTC

Acknodwledgments

This study was carried out at the Molecular Genetics Laboratory, Department of Mathematical and Life Sciences, Graduate School of Science, Hiroshima University. I would like to express my sincere gratitude to my professor, Dr. Takashi Yamamoto, for providing me an understanding enviornment to perform this research as a Ph.D. student. Deep appreciation is also extended to Dr. Naoaki Sakamoto for his patient guidance, considerable encouragement, and invaluable discussions that contributed extensively to this research. I would also like to thank to Dr. Tetsushi Sakuma and Dr. Akinori Awazu for the helpful suggestions and their timely advice.I am grateful to members of Dr. Takashi Yamamoto laboratory for fruitful discussions. I am very grateful to Dr. Masato Kiyomoto (Tateyama Marine Laboratory, Ochanomizu University) for supplying live sea urchins and sea water. Special grade agarose was supplied by GeLBio LLC, Japan. Sequencing analysis was carried out in the Gene Science Division, Natural Science Center for Basic Research and Development, Hiroshima University. This work was partially supported by a Grant-in-Aid for Scientific Research (C) (JSPS KAKENHI Grant Number JP17K07241) to NS.

References

Angerer, L. M., & Angerer, R. C. (2004). Disruption of gene function using antisense morpholinos. *Methods in Cell Biology*, *74*, 699–711.

Becker, W. M., Kleinsmith, L. J., Hardin, J. & Bertoni, G. P. (2003) *The world of the cell*. San Francisco: Benjamin/Cummings Publishing Company.

Barsi, J. C., Tu, Q., Calestani, C., & Davidson, E. H. (2015). Genome-wide assessment of differential effector gene use in embryogenesis. *Development*, *142*, 3892–3901.

Beeble, A., & Calestani, C. (2012). Expression pattern of polyketide synthase-2 during sea urchin development. *Gene Expression Patterns*, *12*, 7–10.

Britten, R. J., Cetta, A., & Davidson, E. H. (1978). The single-copy DNA sequence polymorphism of the sea urchin *Strongylocentrotus purpuratus*. *Cell*, *15*, 1175–1186.

Calestani, C., Rast, J. P., & Davidson, E. H. (2003). Isolation of pigment cell specific genes in the sea urchin embryo by differential macroarray screening. *Development*, *130*, 4587–4596.

Cameron, R. A., Fraser, S. E., Britten, R. J., & Davidson, E. H. (1991). Macromere cell fates during sea urchin development. *Development*, *113*, 1085–1091.

Cameron, R. A., Hough-Evans, B. R., Britten, R. J., & Davidson, E. H. (1987). Lineage and fate of each blastomere of the eight-cell sea urchin embryo. *Genes and Development*, *1*, 75–85.

Castoe, T. A., Stephens, T., Noonan, B. P., & Calestani, C. (2007). A novel group of type I polyketide synthases (PKS) in animals and the complex phylogenomics of PKSs. *Gene*,

392, 47–58.

Cong, L., Ran, F. A., Cox, D., Lin, S., Barretto, R., Habib, N., … Zhang, F. (2013). Multiplex genome engineering using CRISPR/Cas systems. *Science*, *339*, 819–823.

Croce, J. C., & McClay, D. R. (2010). Dynamics of Delta/Notch signaling on endomesoderm segregation in the sea urchin embryo. *Development*, *137*, 83-91.

Davidson, E. H., Rast, J. P., Oliveri, P., Ransick, A., Calestani, C., Yuh, C. H., … Bolouri, H. (2002). A provisional regulatory gene network for specification of endomesoderm in the sea urchin embryo. *Developmental Biology*, *246*, 162–190.

Doudna, J. A., & Charpentier, E. (2014). Genome editing. The new frontier of genome engineering with CRISPR-Cas9. *Science*, *346*, 1258096.

Duboc, V., Röttinger, E., Besnardeau, L., & Lepage, T. (2004). Nodal and BMP2/4 signaling organizes the oral-aboral axis of the sea urchin embryo. *Developmental cell*, *6*, 397-410.

Fu, Y., Foden, J. A., Khayter, C., Maeder, M. L., Reyon, D., Joung, J. K., & Sander, J. D. (2013). High-frequency off-target mutagenesis induced by CRISPR-Cas nucleases in human cells. *Nature Biotechnology*, *31*, 822–826.

Fujiwara, A., & Yasumasu, I. (1997). Does the respiratory rate in sea urchin embryos increase during early development without proliferation of mitochondria? *Development, growth & differentiation*, *39*, 179-189.

Gaj, T., Gersbach, C. A. & Barbas, C. F. (2013) ZFN, TALEN, and CRISPR/Cas-based methods for genome engineering. *Trends in biotechnology*, *31*, 397-405.

Griffiths, M. (1965). A study of the synthesis of naphthaquinone pigments by the larvae of two species of sea urchins and their reciprocal hybrids. *Developmental Biology*, *11*, 433–447.

Hojo, M., Omi, A., Hamanaka, G., Shindo, K., Shimada, A., Kondo, M., … Takeda, H. (2015). Unexpected link between polyketide synthase and calcium carbonate biomineralization. *Zoological Letters*, *1*, 3.

Hopwood, D. A. (1997). Genetic contributions to understanding polyketide synthases. *Chemical Reviews*, *97*, 2465–2498.

Hopwood, D. A., & Sherman, D. H. (1990). Molecular genetics of polyketides and its comparison to fatty acid biosynthesis. *Annual Review of Genetics*, *24*, 37–62.

Horvath, P. & Barrangou, R. (2010) CRISPR/Cas, the immune system of bacteria and archaea. *Science*, *327*, 167-170.

Hosoi, S., Sakuma, T., Sakamoto, N., & Yamamoto, T. (2014). Targeted mutagenesis in sea urchin embryos using TALENs. *Development*, *Growth and Differentiation*, *56*, 92–97.

Hsu, P. D., Scott, D. A., Weinstein, J. A., Ran, F. A., Konermann, S., Agarwala, V., … Zhang, F. (2013). DNA targeting specificity of RNA-guided Cas9 nucleases. *Nature Biotechnology*, *31*, 827–832.

Jiang, W., Bikard, D., Cox, D., Zhang, F., & Marraffini, L. A. (2013). RNA-guided editing of bacterial genomes using CRISPR-Cas systems. *Nature Biotechnology*, *31*, 233–239.

Jinek, M., Chylinski, K., Fonfara, I., Hauer, M., Doudna, J. A., & Charpentier, E. (2012).

A programmable dual-RNA-guided DNA endonuclease in adaptive bacterial immunity. *Science*, *337*, 816–821.

Kim, S., Kim, D., Cho, S. W., Kim, J., & Kim, J. S. (2014). Highly efficient RNA-guided genome editing in human cells via delivery of purified Cas9 ribonucleoproteins. *Genome Research*, *24*, 1012–1019.

Kinjo, S., Kiyomoto, M., Yamamoto, T., Ikeo, K., & Yaguchi, S. (2018). HpBase: A genome database of a sea urchin, *Hemicentrotus pulcherrimus*. *Development*, *Growth and Differentiation*, *60*, 174–182.

Kotani, H., Taimatsu, K., Ohga, R., Ota, S., & Kawahara, A. (2015). Efficient multiple genome modifications induced by the crRNAs, tracrRNA and Cas9 protein complex in zebrafish. *PLoS One*, *10*, e0128319.

Larson, M. H., Gilbert, L. A., Wang, X., Lim, W. A., Weissman, J. S., & Qi, L. S. (2013). CRISPR interference (CRISPRi) for sequence-specific control of gene expression. *Nature Protocols*, *8*, 2180.

Lee, J. S., Kwak, S. J., Kim, J., Kim, A. K., Noh, H. M., Kim, J. S., & Yu, K. (2014). RNA-guided genome editing in Drosophila with the purified Cas9 protein. *G3*: *Genes*, *Genomes*, *Genetics*, *4*, 1291–1295.

Lee, P. Y., & Davidson, E. H. (2004). Expression of Spgatae, the Strongylocentrotus purpuratus ortholog of vertebrate GATA4/5/6 factors. *Gene Expression Patterns*, *5*, 161-165.

Lee, P. Y., Nam, J., & Davidson, E. H. (2007). Exclusive developmental functions of gatae cis-regulatory modules in the Strongylocentrorus purpuratus embryo. *Developmental biology*, *307*, 434-445.

Lin, C. Y., & Su, Y. H. (2016). Genome editing in sea urchin embryos by using a CRISPR/Cas9 system. *Developmental Biology*, *409*, 420–428.

Materna, S. C., Nam, J., & Davidson, E. H. (2010). High accuracy, high-resolution prevalence measurement for the majority of locally expressed regulatory genes in early sea urchin development. *Gene Expression Patterns*, *10*, 177-184.

Materna, S. C., Ransick, A., Li, E., & Davidson, E. H. (2013). Diversification of oral and aboral mesodermal regulatory states in pregastrular sea urchin embryos. *Developmental biology*, *375*, 92-104.

Mellott, D. O., Thisdelle, J., & Burke, R. D. (2017). Notch signaling patterns neurogenic ectoderm and regulates the asymmetric division of neural progenitors in sea urchin embryos. *Development*, *144*, 3602–3611.

Minokawa, T., Rast, J. P., Arenas-Mena, C., Franco, C. B., & Davidson, E. H. (2004). Expression patterns of four different regulatory genes that function during sea urchin development. *Gene Expression Patterns*, *4*, 449-456.

Naito, Y., Hino, K., Bono, H., & Ui-Tei, K. (2014). CRISPRdirect: software for designing CRISPR/Cas guide RNA with reduced off-target sites. *Bioinformatics*, *31*, 1120-1123.

Nakayama, T., Blitz, I. L., Fish, M. B., Odeleye, A. O., Manohar, S., Cho, K. W., & Grainger, R. M. (2014). Cas9-based genome editing in *Xenopus tropicalis*. In J. A. Doudna & E. J. Sontheimer (Eds.), *Methods in enzymology* (Vol. 546, pp. 355–375). Cambridge, MA: Academic Press.

Ochiai, H., Fujita, K., Suzuki, K. I., Nishikawa, M., Shibata, T., Sakamoto, N., & Yamamoto, T. (2010). Targeted mutagenesis in the sea urchin embryo using zinc-finger

nucleases. *Genes to Cells*, *15*, 875–885.

Okabayashi, K., & Nakano, E. (1983). The cytochrome system of sea urchin eggs and embryos. *Archives of biochemistry and biophysics*, *225*, 271-278.

Oliveri, P., & Davidson, E. H. (2004). Gene regulatory network controlling embryonic specification in the sea urchin. *Current Opinion in Genetics and Development*, *14*, 351–360.

Oliveri, P., Tu, Q., & Davidson, E. H. (2008). Global regulatory logic for specification of an embryonic cell lineage. *Proceedings of the National Academy of Sciences of the United States of America*, *105*, 5955–5962.

Oulhen, N., Swartz, S. Z., Laird, J., Mascaro, A., & Wessel, G. M. (2017). Transient translational quiescence in primordial germ cells. *Development*, *144*, 1201–1210.

Oulhen, N., & Wessel, G. M. (2016). Albinism as a visual, in vivo guide for CRISPR/Cas9 functionality in the sea urchin embryo. *Molecular Reproduction and Development*, *83*, 1046–1047.

Peterson, R. E., & McClay, D. R. (2005). A Fringe-modified Notch signal affects specification of mesoderm and endoderm in the sea urchin embryo. *Developmental biology*, *282*, 126-137.

Ransick, A., & Davidson, E. H. (2006). cis-regulatory processing of Notch signaling input to the sea urchin glial cells missing gene during mesoderm specification. *Developmental biology*, *297*, 587-602.

Ransick, A., & Davidson, E. H. (2012). Cis-regulatory logic driving glial cells missing: self-sustaining circuitry in later embryogenesis. *Developmental biology*, *364*, 259-267.

Rast, J. P. (2000). Transgenic manipulation of the sea urchin embryo. *Methods in Molecular Biology*, *136*, 365–373.

Sakane, Y., Iida, M., Hasebe, T., Fujii, S., Buchholz, D. R., Ishizuya-Oka, A., … Kenichi, T. S. (2018). Functional analysis of thyroid hormone receptor beta in *Xenopus tropicalis* founders using CRISPR-Cas. *Biology Open*, *7*, bio030338.

Sakane, Y., Suzuki, T. S., & Yamamoto, T. (2017). A simple protocol for loss-of-function analysis in *Xenopus tropicalis* founders using the CRISPR-cas system. In I. Hatada (Ed.), *Genome editing in animals* (pp. 189–203). New York, NY: Humana Press.

Sea Urchin Genome Sequencing Consortium (2006). The genome of the sea urchin *Strongylocentrotus purpuratus*. *Science*, *314*, 941–952.

Shevidi, S., Uchida, A., Schudrowitz, N., Wessel, G. M., & Yajima, M. (2017). Single nucleotide editing without DNA cleavage using CRISPR/Cas9-deaminase in the sea urchin embryo. *Developmental Dynamics*, *246*, 1036–1046.

Shigeta, M., Sakane, Y., Iida, M., Suzuki, M., Kashiwagi, K., Kashiwagi, A., … Suzuki, K. I. T. (2016). Rapid and efficient analysis of gene function using CRISPR-Cas9 in *Xenopus tropicalis* founders. *Genes to Cells*, *21*, 755–771.

Smith, M. M., Cruz Smith, L., Cameron, R. A., & Urry, L. A. (2008). The larval stages of the sea urchin, *Strongylocentrotus purpuratus*. *Journal of Morphology*, *269*, 713–733.

Staunton, J., & Weissman, K. J. (2001). Polyketide biosynthesis: A millennium review. *Natural Product Reports*, *18*, 380–416.

Sung, Y. H., Kim, J. M., Kim, H. T., Lee, J., Jeon, J., Jin, Y., … Lee, H. W. (2014). Highly efficient gene knockout in mice and zebrafish with RNA-guided endonucleases. *Genome*

Research, *24*, 125–131.

Yamaguchi, M., Kinoshita, T., & Ohba, Y. (1994). Fractionation of Micromeres, Mesomeres, and Macromeres of 16-cell Stage Sea Urchin Embryos by Elutriation. *Development, Growth & Differentiation*, *36*, 381-387.

Yamamoto, T., Kawamoto, R., Fujii, T., Sakamoto, N., & Shibata, T. (2007). DNA variations within the sea urchin Otx gene enhancer. *FEBS Letters*, *581*, 5234–5240

Zhu, X., Xu, Y., Yu, S., Lu, L., Ding, M., Cheng, J., … Meng, S. (2014). An efficient genotyping method for genome-modified animals and human cells generated with CRISPR/Cas9 system. *Scientific Reports*, *4*, 6420.